

Synthesis of hydroxyapatite by hydrolysis of α - $\text{Ca}_3(\text{PO}_4)_2$

O. V. Sinitsyna,^a A. G. Veresov,^a E. S. Kovaleva,^a Yu. V. Kolen'ko,^a V. I. Putlyaev,^{b*} and Yu. D. Tretyakov^{a,b}

M. V. Lomonosov Moscow State University,

^aDepartment of Materials Science,

^bDepartment of Chemistry,

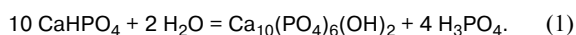
1 Leninskie Gory, 119992 Moscow, Russian Federation.

Fax: +7 (095) 939 0998. E-mail: putl@inorg.chem.msu.ru

Conditions for hydroxyapatite (HAP) synthesis in aqueous solutions by hydrolysis of α - $\text{Ca}_3(\text{PO}_4)_2$ were studied. Temperature exerts a substantial effect on the rate of α - $\text{Ca}_3(\text{PO}_4)_2$ hydrolysis and also changes the morphology of the reaction products. At 40 °C, the plate-like intersecting (perpendicular to the surface of the initial particles) crystals of HAP grow. Their maximum size after the 24-h hydrolysis is 1–2 μm . Needle-like HAP crystals are formed upon boiling of the suspension. The morphology observed for the HAP particles agrees well with the conclusions obtained by analysis of the kinetics of tricalcium phosphate hydrolysis.

Key words: biomaterials, hydroxyapatite, calcium orthophosphates, hydrolysis.

Materials based on hydroxyapatite $\text{Ca}_{10-x}(\text{HPO}_4)_x(\text{PO}_4)_{6-x}(\text{OH})_{2-x}$ (HAP, $x = 0-1$) find wide use in modern medicine for recovering bone defects due to their high biological compatibility with tissues of living organisms.¹⁻⁴ Hydrolysis of calcium orthophosphates is one of the most important methods for hydroxyapatite synthesis in aqueous solutions.^{1,2,5-18} Hydrolysis reactions reproduce better the composition and morphology of synthesized hydroxyapatite crystals than precipitation processes due to a smaller number of synthesis parameters (temperature, reaction duration, ratio and composition of the starting reagents, and pH). Hydroxyapatite can be synthesized by the hydrolysis of both individual phosphates, such as $\text{CaHPO}_4 \cdot 2\text{H}_2\text{O}$, CaHPO_4 , α - $\text{Ca}_3(\text{PO}_4)_2$, β - $\text{Ca}_3(\text{PO}_4)_2$, $\text{Ca}_8\text{H}_2(\text{PO}_4)_6 \cdot 5\text{H}_2\text{O}$, and $\text{Ca}_4(\text{PO}_4)_2\text{O}$, and their mixtures.^{1,2} An important parameter of the hydrolysis of calcium orthophosphates is the stoichiometry of the initial compound. The hydrolysis of calcium phosphates with $\text{Ca}/\text{P} < 1.67$ is accompanied by accumulation of an acid as the reaction product and, as a consequence, by the fast inhibition of the reaction²



In the case of $\text{Ca}_3(\text{PO}_4)_2$, hydrolysis can occur to completeness and form nonstoichiometric hydroxyapatite as the single product^{2,5-16}



The formation of stoichiometric HAP can be expected in a highly alkaline medium



Table 1. Solubility of calcium phosphates³

Compounds	Ca/P	-log K_S^*	
		25 °C	37 °C
$\text{Ca}_{10}(\text{PO}_4)_6(\text{OH})_2$	1.67	116.8	117.2
α - $\text{Ca}_3(\text{PO}_4)_2$	1.5	25.5	—
β - $\text{Ca}_3(\text{PO}_4)_2$	1.5	28.9	29.5

* K_S is the solubility product.

Two modifications of tricalcium phosphate are known: low-temperature β - $\text{Ca}_3(\text{PO}_4)_2$ (exists below 1100 °C) and high-temperature α - $\text{Ca}_3(\text{PO}_4)_2$.³ The solubility of the low-temperature modification is higher than that of hydroxyapatite but lower than the solubility of the high-temperature α -modification (Table 1).³ Therefore, β - $\text{Ca}_3(\text{PO}_4)_2$ is used as a component of the resorbable bioceramics, whose rate of dissolution in biological liquids of an organism corresponds to the rate of formation of a new bone tissue, *i.e.*, the newly formed bone tissue has time to substitute the dissolved material. The α - $\text{Ca}_3(\text{PO}_4)_2$ modification finds wide use for the preparation of calcium phosphate cements, *viz.*, materials prepared by the setting of powdered mixtures blended with a small amount of water due to hydrolysis reactions.^{1,2} The high biological compatibility of the material with tissues is considered¹ to be caused by both chemical and morphological similarity of the synthetic HAP and bone apatite. The bone biomineral is nonstoichiometric, because its Ca/P ratio is ~ 1.5 , its crystals being planar prisms $60 \times 20 \times 5$ nm in size.

Published data on the rate of α -tricalcium phosphate transformation into hydroxyapatite and morphology

of the resulting crystals are contradictory. The early works^{5–7} reported a low rate of hydrolysis at $T \leq 40$ °C (<5% conversion for 3 h), which is explained by the heterogeneous character of the process: the reaction rate decreases as a product layer is formed on the surface of the initial α - $\text{Ca}_3(\text{PO}_4)_2$ particles. In some cases,^{5,9–11} the hydrolysis of α - $\text{Ca}_3(\text{PO}_4)_2$ was relatively fast (100% conversion for 48 h at 30 °C and for 2 h at 75 °C). The data on the morphology of hydroxyapatite synthesized by α - $\text{Ca}_3(\text{PO}_4)_2$ hydrolysis differ strongly: joints of plate-like crystals with a size (in the plane) of 1–5 μm are formed most frequently.^{5,6,9–11} The authors of Ref. 11 believe that the growth of planar crystals perpendicularly to the surface of primary particles create no substantial diffusion hindrance for the reaction as the product accumulates. The hydrolysis of α - $\text{Ca}_3(\text{PO}_4)_2$ occurs noticeably even in the presence of hydroxyapatite "seeds,"⁶ *i.e.*, nucleation is the rate-determining step of the reaction.

According to published data,^{9–11} at $T > 70$ °C the rate of α - $\text{Ca}_3(\text{PO}_4)_2$ hydrolysis increases substantially. Higher temperatures (>100 °C) would enhance the formation rate of hydroxyapatite during the hydrolysis of α -tricalcium phosphate. However, the hydrothermal treatment of powders of calcium phosphates for the preparation of hydroxyapatite have not virtually been reported until recently.^{15–17} The synthesis temperature can also determine the morphology of particles: needle-like HAP crystals are obtained, as a rule, in hot aqueous solutions. Such crystals find use for the reinforcement of biologically compatible composites to improve their strength characteristics.

Thus, the following practically significant parameters should be taken into account when considering the reactions of α - $\text{Ca}_3(\text{PO}_4)_2$ hydrolysis: (1) rate of hydrolysis to form HAP and (2) size and shape of the crystals formed. The conditions for preparing the HAP crystals with a specified morphology during an appropriate time (several hours) cannot be chosen unambiguously on the basis of available published data. In this work, we studied the effect of the synthesis temperature on the rate of α - $\text{Ca}_3(\text{PO}_4)_2$ hydrolysis processes and morphology of the resulting crystals.

Experimental

Calcium carbonate CaCO_3 (reagent grade) and calcium hydrophosphate CaHPO_4 (reagent grade) or calcium pyrophosphate $\text{Ca}_2\text{P}_2\text{O}_7$ (analytical grade) taken in the ratios $\text{Ca}/\text{P} = 1.5$ and 1.55 were used for the synthesis of α - $\text{Ca}_3(\text{PO}_4)_2$. After triturating in a mortar, a mixture of the substances was annealed in air for 3 h at 1300 °C



After high-temperature treatment, the samples were quenched in air to prevent the formation of an admixture of the low-temperature β -modification or were cooled in the furnace.

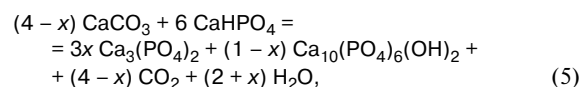
The resulting powders were triturated in an agate mortar for 15 min. During hydrolysis, the temperatures of suspensions containing an α - $\text{Ca}_3(\text{PO}_4)_2$ powder (0.5 g) in distilled water (100 mL) were maintained at 20, 40, 60, and 100 °C. The suspensions with the same solid phase to water ratio were ultrasonicated on an UZDN-A ultrasonic dispergator (radiation power 35 W/100 cm^3 , frequency 30 kHz) for 1 h at 20 °C. The hydrothermal treatment of suspensions containing $\text{Ca}_3(\text{PO}_4)_2$ (0.5 g) in water (40 mL) was carried out at 150, 175, and 200 °C for 2–5 h in a specially designed autoclave.¹⁸ The powders obtained were filtered, washed with distilled water and acetone, and dried in air. To study the effect of the ionic strength (I) on the morphology of the HAP crystals, we hydrolyzed α - $\text{Ca}_3(\text{PO}_4)_2$ in an autoclave at 200 °C in solutions of NaCl ($I = 150$ mmol L^{-1}).

The synthesized substances were studied by X-ray diffraction analysis in the interval of angles $2\theta = 10$ – 60° (Cu- $K\alpha$ radiation, Dron-3M, Russia) and IR spectroscopy in the 400–4000 cm^{-1} range (pellets: 1 mg of powder in 150 mg of KBr (analytical grade, $d = 13$ mm, Perkin–Elmer 1600 FTIR spectrophotometer, USA). The micromorphology of the powders was studied by scanning electron microscopy (JEM-2000FX II (Jeol), Japan, accelerating voltage 200 kV and Leo Supra 50VP, Germany, 5 kV). The kinetics of the initial steps of reactions (2) and (3) was studied by a change in the pH of an aqueous suspension of $\text{Ca}_3(\text{PO}_4)_2$ at room temperature (Ekspert-001 ionometer, Ekoniks, Russia). To plot the solubility isotherms and calculate the conversion (α) in hydrolytic reactions, ion equilibria in solutions were calculated using the PHREEQC for Windows, v.1.5.10 computer program for geochemical calculations of low-temperature reactions in aqueous media.¹⁹

Results and Discussion

According to the X-ray diffraction data, the α - $\text{Ca}_3(\text{PO}_4)_2$ samples prepared by reaction (4) upon cooling in a furnace contained up to 15 wt.% of the low-temperature β - $\text{Ca}_3(\text{PO}_4)_2$ modification. The single-phase samples were obtained only by the fast quenching of the samples in air. The X-ray diffraction data show that the composition of the powders obtained by the high-temperature annealing of CaCO_3 and CaHPO_4 depends on the Ca/P ratio in the initial mixture (Fig. 1). An admixture of hydroxyapatite (about 25 wt.%) was found in the samples along with the main synthesis product α - $\text{Ca}_3(\text{PO}_4)_2$ when the Ca/P value changed from 1.5 to 1.55.

We can propose the scheme of the process, according to which a multiphase mixture is formed in the system with the starting Ca/P ratio $\text{Ca}/\text{P} > 1.5$



where $0 < x < 1$. The dependence of the phase composition of the final mixture on its overall stoichiometry (Ca/P) is expressed by the equation

$$\text{Ca}/\text{P} = (10-x)/6. \quad (6)$$

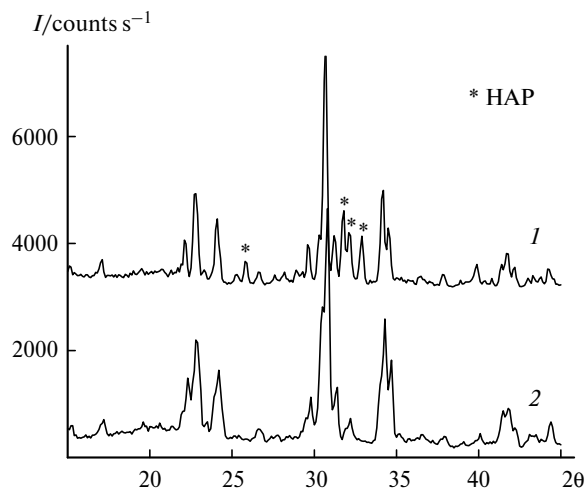
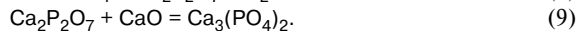


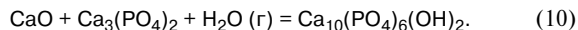
Fig. 1. XRD patterns of the samples prepared in the synthesis of α - Ca_3PO_4 via reaction (5) (I is intensity/counts s^{-1}): Ca/P = 1.55 (1) and 1.5 (2).

For the ratio Ca/P = 1.55, $x = 0.7$, which corresponds, according to the calculation by Eq. (5), to the composition of the final mixture of 32 wt.% HAP and 68% $\text{Ca}_3(\text{PO}_4)_2$. Thus, even an insignificant deviation of the starting mixture from the required stoichiometry Ca/P = 1.5 during the synthesis of α - $\text{Ca}_3(\text{PO}_4)_2$ exerts a substantial effect on the composition of the final product: pure tricalcium phosphate or a mixture of $\text{Ca}_3(\text{PO}_4)_2$ and HAP.

The real mechanism of formation of a $\text{Ca}_3(\text{PO}_4)_2$ –HAP mixture is much more complex than reaction (5); the reaction route in the phosphate–carbonate mixture considered includes several steps. According to the previously published data,^{17,20} which were confirmed by the present study, calcium oxide and pyrophosphates are intermediate products of the $\text{Ca}_3(\text{PO}_4)_2$ synthesis and formed by the following reactions:



It can be assumed that the formation of an HAP admixture by cooling of the samples calcined at 1300 °C and containing local excess calcium with respect to phosphorus is described by the equation



Since the involvement of the air moisture is assumed, one should expect that the main portion of the HAP admixture is formed on the surface of the main reaction product, *viz.*, α - $\text{Ca}_3(\text{PO}_4)_2$.

According to the electron microscopy data, a powder with particles $\leq 10 \mu\text{m}$ in size (Fig. 2) was obtained by the synthesis of tricalcium phosphate. A considerable amount of particles of the new phase with sizes $< 0.3 \mu\text{m}$ (see

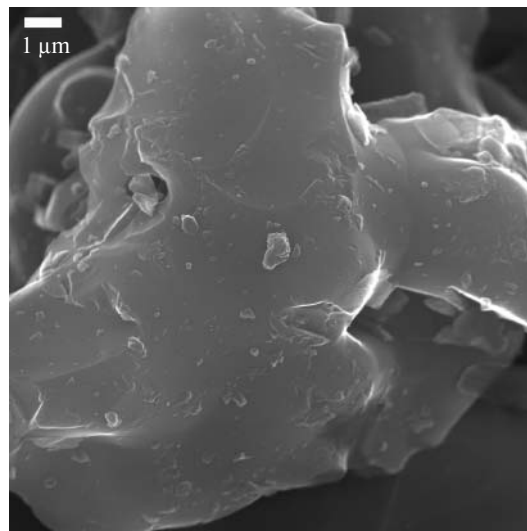


Fig. 2. Microphotograph of an α - $\text{Ca}_3(\text{PO}_4)_2$ particle containing hydroxyapatite precipitates on the surface.

Fig. 2) presumably corresponding to HAP was detected by the microscopic study of the surface of the $\text{Ca}_3(\text{PO}_4)_2$ crystals obtained by the above-described method. The formation of a hydroxyapatite layer on the $\text{Ca}_3(\text{PO}_4)_2$ particle surface should prevent their further hydrolysis, which is confirmed in this study.

Two routes of β - $\text{Ca}_3(\text{PO}_4)_2$ hydrolysis can be proposed (see Eqs (2) and (3)). Both stoichiometric and nonstoichiometric HAP can be formed, depending on the reaction route.

Based on the data for ion equilibria simulation in the $\text{Ca}_{10}(\text{PO}_4)_6(\text{OH})_2$ – H_2O and $\text{Ca}_3(\text{PO}_4)_2$ – H_2O systems, we plotted the solution composition (with respect to calcium and phosphate ions) vs. acidity of the medium at 25 °C, namely, the solubility isotherms (Fig. 3, *a, b*). The isotherms show the change in the composition of the solution (with respect to a certain ion, calcium cation or phosphate anion) equilibrated with a certain phase at different pH. Any point below the corresponding isotherm corresponds to the composition of a solution supersaturated relatively to this calcium phosphate. The higher the isotherm of calcium phosphate in the diagram, the more thermodynamically stable this phase compared to other calcium phosphates, whose isotherms lie below. It can be seen that an aqueous solution contacting with α - $\text{Ca}_3(\text{PO}_4)_2$ is strongly supersaturated relatively to hydroxyapatite in the whole interval of the pH values of hydrolysis (Fig. 4).

The higher starting pH value corresponds to the samples for which the dissolution processes in the initial step prevail over the hydrolysis processes (Fig. 5).

According to the X-ray diffraction data, for the initially heterophase samples, whose considerable part of the granule surface is covered with an HAP layer, at $T \leq 40 \text{ }^\circ\text{C}$

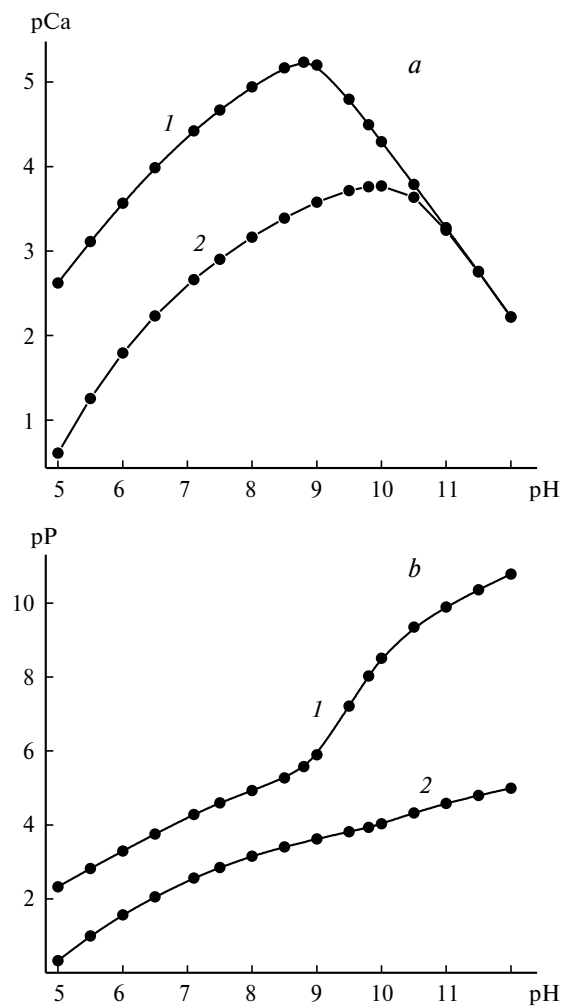


Fig. 3. Solubility isotherms of HAP (1) and α -Ca₃(PO₄)₂ (2) in the coordinates pCa (a) and pP (b) at 25 °C; pCa ($\equiv -\log[\text{Ca}^{2+}]$)—pH; pP ($\equiv -\log([\text{HPO}_4^{2-}] + [\text{PO}_4^{3-}])$)—pH.

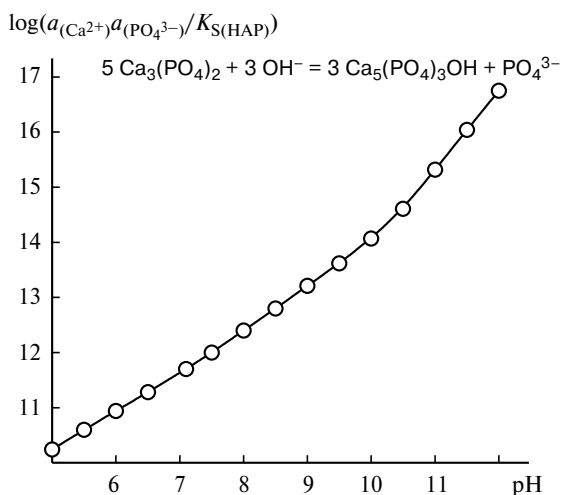


Fig. 4. Supersaturation of a solution equilibrated with α -Ca₃(PO₄)₂ relatively to HAP at different pH.

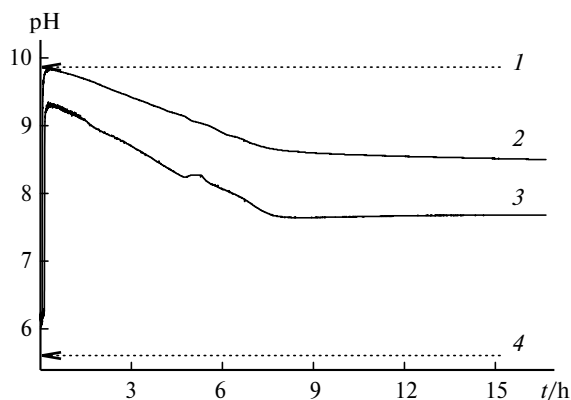


Fig. 5. Change in the pH of suspensions of α -Ca₃(PO₄)₂: 1, pH of a solution equilibrated with α -Ca₃(PO₄)₂; 2, initial sample of α -Ca₃(PO₄)₂ + 25% HAP; 3, initial sample of α -Ca₃(PO₄)₂; and 4, pH of a solution after the complete hydrolysis of Ca₃(PO₄)₂ with the formation of Ca₁₀(PO₄)₆(OH)₂.

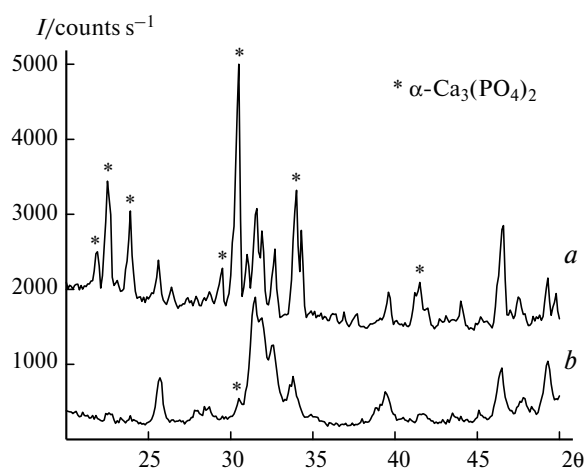


Fig. 6. XRD patterns of the samples synthesized by hydrolysis at 40 °C for 1 day: single-phase sample of α -Ca₃(PO₄)₂ (a) and the sample with 25% HAP (b).

hydrolysis is very slow (Fig. 6). The hydrolysis rate of pure α -Ca₃(PO₄)₂ increases considerably with temperature: the 100% conversion is achieved within 48 h at 40 °C and within 3 h at 100 °C. At 100 °C, after the 30-min hydrolysis, more than 50 wt.% Ca₃(PO₄)₂ are transformed into HAP.

The time plots of the conversion of α -Ca₃(PO₄)₂ to HAP by reaction (3) during the low-temperature hydrolysis of α -Ca₃(PO₄)₂ were obtained by measurements of the pH of the suspensions (see Fig. 5). The pH values of solutions with different initial pH values equilibrated with α -Ca₃(PO₄)₂ (initial state, $\alpha = 0$) and equilibrated with HAP (final state, $\alpha = 1$) were calculated by the constants of ion and heterogeneous equilibria using the PHREEQC program. For the high-temperature hydrolysis (at 100 °C), the time plot of the conversion was obtained from the

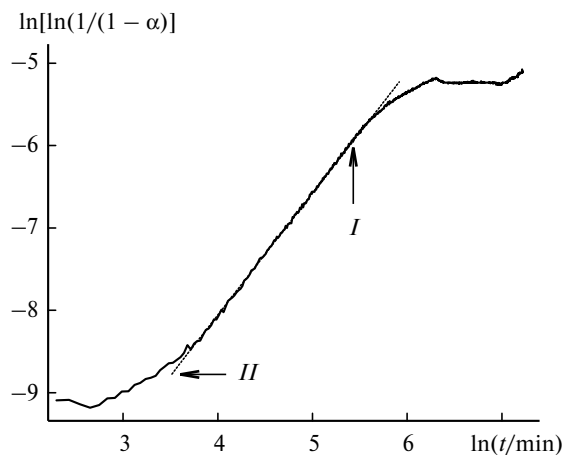


Fig. 7. Kinetic curves of the hydrolysis of α -Ca₃(PO₄)₂ at 20 °C (in the Kolmogorov—Avrami coordinates): *I*, maximum reaction rate and *II*, $\ln[\ln(1/(1-\alpha))] = -(13.96 \pm 0.01) + (1.48 \pm 0.02)\ln t$.

data on the quantitative X-ray analysis of the composition of the powders taken at different moments. The kinetics of α -Ca₃(PO₄)₂ hydrolysis in the temperature range from 20 to 100 °C was studied using the Kolmogorov—Avrami equation (Fig. 7)

$$-\ln(1-\alpha) = \kappa t^n, \quad (11)$$

where α is the conversion of α -Ca₃(PO₄)₂ to HAP during hydrolysis, t is the hydrolysis time (min), and n is the exponent in the kinetic equation (positive number characterizing the reaction mechanism).

Equation (11) is used due to its universal character: it is fulfilled, as a rule, in a wide range of conversions $0.05 < \alpha < 0.9$. The boundaries of its application are presently much broader than those primarily proposed by the authors of the model. For diffusion-controlled reactions, the exponent is $n = \beta + \lambda/2$ (β is the parameter characterizing the nucleation rate: $\beta = 0$ for instant nucleation, $\beta = 1$ for nucleation with a constant rate, and $0 < \beta < 1$ for inhibited nucleation; λ is the number of directions of the nuclei growth). For reactions with a constant rate of interface motion, $n = \beta + \lambda$.²¹ Sometimes the reaction mechanism cannot be elucidated because of many combinations of λ and β , although the n value is determined. Therefore, additional data are needed, for instance, the results of direct microscopic observations. Nevertheless, it is seen that for diffusionally controlled reactions $0.5 \leq n \leq 2.5$, and for reactions with kinetic control $1 \leq n \leq 4$. According to the electron microscopy data, hydrolysis produces needle- or plate-like particles corresponding to $\lambda = 1$ and 2, respectively (Fig. 8). For example, the hydrolysis kinetics at 100 °C gave the exponent $n = 0.5$, and the product particles are needle-like ($\lambda = 1$). From this we concluded that the reaction occurs in the diffusion regime with the instant nucleation of the product ($\beta = 0$). The study of the reaction kinetics at

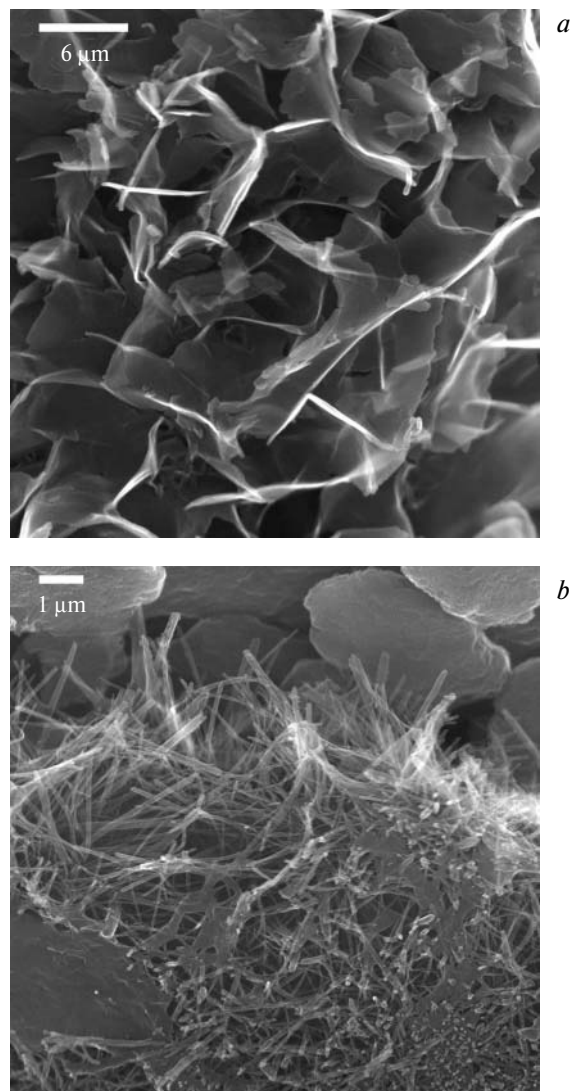


Fig. 8. SEM microphotographs of the HAP crystals synthesized by α -Ca₃(PO₄)₂ hydrolysis at 40 °C for 24 h (*a*) and at 100 °C for 30 min (*b*).

25 °C gave $n = 1.5$, and the reaction product was predominantly plate-like ($\lambda = 2$). The product of similar morphology can be formed at this exponent n in the kinetic equation only in a diffusion-controlled reaction with an inhibited nucleation rate ($\beta = 0.5$).

Several mechanisms of Ca₃(PO₄)₂ hydrolysis have been proposed. One of them²² is based on the crystallochemical resemblance of HAP and α -Ca₃(PO₄)₂, which are often described as a pile of cation-cationic and cation-anionic columns. The hydrolysis is described as the diffusion of H⁺ and OH⁻ ions formed due to water ionization producing the Ca₃(PO₄)₂ structure. As a result, the structure of nonstoichiometric hydroxyapatite "Ca₉H(PO₄)₆OH" is formed, in which some calcium positions are occupied by protons, and the remaining hydroxyl groups form channels along the *c* axis of the cell. This description is not

valid. It is more probable that hydrolysis proceeds *via* the mechanism "dissolution of $\text{Ca}_3(\text{PO}_4)_2$ —precipitation of HAP." This is also favored by the relatively high solubility of $\alpha\text{-Ca}_3(\text{PO}_4)_2$ (see Table 1). The crystallochemical similarity of the structures should undoubtedly facilitate the epitaxial HAP growth on the $\text{Ca}_3(\text{PO}_4)_2$ particle surface. This fact indicates that the energy barrier of rearrangement of the $\text{Ca}_3(\text{PO}_4)_2$ structure to HAP is low (and, hence, the activation energy of motion of the $\text{Ca}_3(\text{PO}_4)_2$ /HAP interface, which is comparable with the energy barrier, is also low). Hydroxyapatite was shown¹⁶ to crystallize through the formation of an amorphous layer on the tricalcium phosphate surface. The composition of amorphous calcium phosphate (ACP), which is a metastable phase (HAP precursor in aqueous solutions), is often described by the formula $\text{Ca}_9(\text{PO}_4)_6 \cdot x\text{H}_2\text{O}$ ($\text{Ca}/\text{P} = 1.5$). At the same time, HAP as a phase exists in the interval of stoichiometric ratios $1.5 \leq \text{Ca}/\text{P} \leq 1.67$, and an increase in the pH and elongation of the synthesis time favor an increase in the Ca/P value.¹⁷ Thus, when the ACP layer precipitated on the $\text{Ca}_3(\text{PO}_4)_2$ particle surface is crystallized, the solution adjacent to this layer is systematically depleted in the Ca^{2+} and OH^- ions. This induces a diffusion flow of the corresponding ions from the solution bulk to the ACP/solution interface. There is no contradiction

to our conclusion about the diffusion-controlled character of $\text{Ca}_3(\text{PO}_4)_2$ hydrolysis. We can also assert that the surface of the initial particles (composition and microstructure) are very significant for the hydrolysis of $\text{Ca}_3(\text{PO}_4)_2$. The formation of an HAP admixture on the $\text{Ca}_3(\text{PO}_4)_2$ particle surface because of the violation of the initial Ca/P stoichiometry decreases the flow of the Ca^{2+} and PO_4^{3-} ions directed from the surface to solution due to the dissolution of $\text{Ca}_3(\text{PO}_4)_2$ and, in addition, prevents ACP layer formation during ion precipitation from solution on the particle surface. This decreases the hydrolysis rate of the heterophase $\text{Ca}_3(\text{PO}_4)_2$ samples compared to the pure phase.

The temperature is an important parameter of the synthesis and affects substantially the rate of $\text{Ca}_3(\text{PO}_4)_2$ hydrolysis, along with changing the morphology of the reaction products. Boiling of the $\text{Ca}_3(\text{PO}_4)_2$ suspension produces HAP crystals of the needle-like (filament) shape with the length about $5 \mu\text{m}$ and diameter $\leq 100 \text{ nm}$ (see Figs 8 and 9, *a*). The crystal growth occurs from the surface of tricalcium phosphate particles.

The hydrolysis of $\text{Ca}_3(\text{PO}_4)_2$ is inhibited, because a product layer is formed on the particle surface. An attempt to intensify $\text{Ca}_3(\text{PO}_4)_2$ hydrolysis by the ultrasonication of the system was unsuccessful, because the

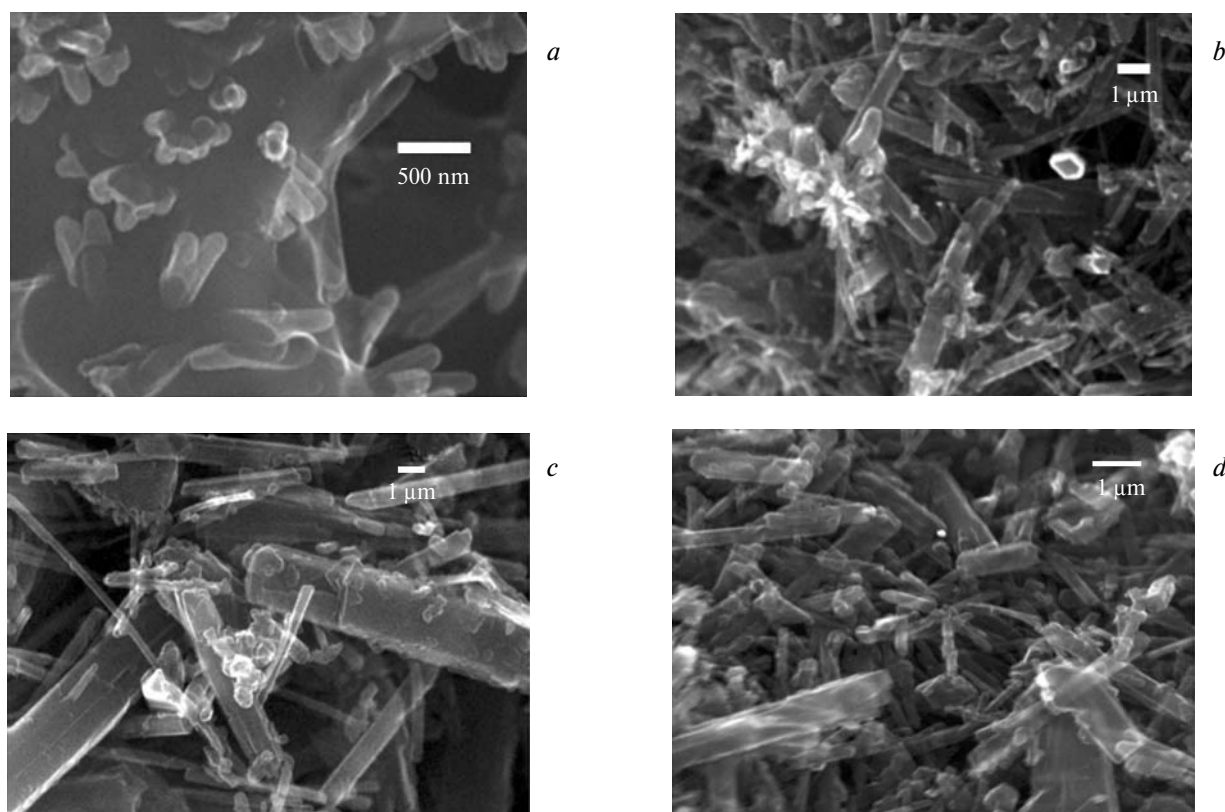


Fig. 9. SEM microphotographs of the HAP samples synthesized by $\alpha\text{-Ca}_3(\text{PO}_4)_2$ hydrolysis at $60 \text{ }^\circ\text{C}$ for 3 h (*a*), $175 \text{ }^\circ\text{C}$ for 5 h (*b*), $200 \text{ }^\circ\text{C}$ for 5 h (*c*), and $200 \text{ }^\circ\text{C}$ for 5 h (*d*) in a 150 mM solution of NaCl.

conversion of Ca₃(PO₄)₂ to HAP obtained by this treatment was the same as that in the case of an increase in the hydrolysis temperature. Thus, the driving force of the ultrasonic treatment was only the heating of the solution due to cavitation. Nevertheless, we believe that a powerful ultrasonication can exert a significant effect on the hydrolytic reaction (due to the renewal of the reaction surface and more efficient stirring of the solution), namely, the diffusion regime of hydrolysis. Another approach used in this work to accelerate the reaction was the hydrothermal treatment of the heterophase Ca₃(PO₄)₂–HAP samples at 150, 175, and 200 °C.

The hydrothermal synthesis of HAP from α -Ca₃(PO₄)₂ at 150–200 °C affords large rod-like crystals (see Table 2, Fig. 9). The characteristic shape of the crystals (hexagonal needles) is distorted, indicating that the hydroxyapatite crystals grow under nonequilibrium conditions. The increase in the average crystal size with the temperature increase and elongation of the treatment duration ($d \sim 0.6 \mu\text{m}$ at 150 °C and $d \sim 1\text{--}2 \mu\text{m}$ at 200 °C, 5 h) is due to the recrystallization of the initial hydroxyapatite needles. In solutions with a higher ionic strength (150 mM solution of NaCl), the crystal growth is suppressed because of a decrease in the ion activities (see Fig. 9, *c*, *d*).

The IR spectra of the hydrothermally treated Ca₃(PO₄)₂ samples are almost identical and correspond to hydroxyapatite Ca_{10–x/2}(CO₃)_x(PO₄)_{6–x}(OH)₂ (Fig. 10). The IR spectra contain weak absorption bands at ~ 875 and 1420 cm^{-1} corresponding to vibrations of the carbonate anion. In this case, the starting solution can be a source of the carbonate anion, because water was not specially purified from dissolved carbon dioxide.

Thus, the hydrolysis rate of α -Ca₃(PO₄)₂ with an HAP admixture decreases with an increase in the degree of phase heterogeneity of the material. An increase in the hydrolysis temperature changes the HAP morphology from plate-like (at 40 °C) to needle-like (at 100 °C) for the HAP crystals 0.5–5 μm in size. Materials with the

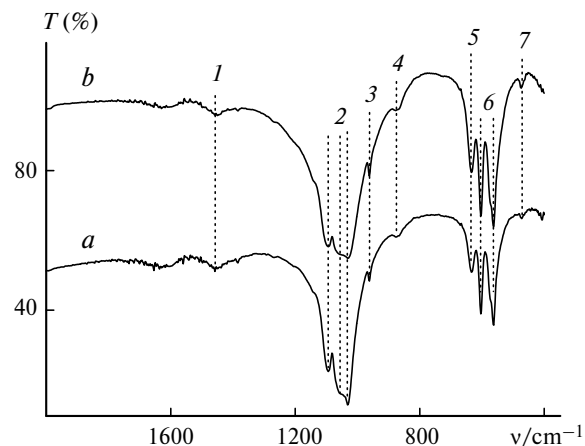


Fig. 10. IR spectra of the HAP samples prepared by the hydrothermal treatment of Ca₃(PO₄)₂ at 175 °C for 5 h (*a*) and at 200 °C for 2 h (*b*): 1, $\nu_4(\text{CO}_3^{2-})$; 2, $\nu_3(\text{PO}_4^{3-})$; 3, $\nu_1(\text{PO}_4^{3-})$; 4, $\nu_3(\text{CO}_3^{2-})$; 5, $\nu_1(\text{OH}^-)$; 6, $\nu_4(\text{PO}_4^{3-})$; and 7, $\nu_2(\text{PO}_4^{3-})$.

submicronic particle size are preferential for practical use. The growth of bioactive nanocrystals requires low temperatures of the synthesis, which inhibits substantially the hydrolysis of α -Ca₃(PO₄)₂: 100% conversion for 48 h at 40 °C and for 3 h at 100 °C. Relatively large elongated particles prepared by high-temperature hydrolysis can be used for the creation of composite biomaterials. Hydroxyapatite powders with controlled bioactivity can be obtained by the variation of the particle size in a wide interval.

This work was financially supported by the Russian Foundation for Basic Research (Program of Support for Leading Scientific Schools of Russia, Grant NSh-2033.03.2003), the Russian Foundation for Basic Research (Project Nos. 02-03-33271b and 03-03-42524-z), the Ministry of Science and Education (Program "Universities of Russia," Grant UR.06.03.006), and the M. V. Lomonosov Moscow State University (Interdisciplinary Research Project No. 26).

References

1. W. Suchanek and M. Yashimura, *J. Mater. Res.*, 1998, **13**, 94.
2. E. Fernandez, F. J. Gil, M. P. Ginebra, F. C. M. Driessens, J. A. Planell, and S. M. Best, *J. Mater. Sci.: Materials in Medicine*, 1999, **10**, 169.
3. S. V. Dorozhkin and M. Epple, *Angew. Chem., Int. Ed.*, 2002, **41**, 3130.
4. M. Vallet-Regi, *J. Chem. Soc., Dalton Trans.*, 2000, 97.
5. M. P. Ginebra, E. Fernandez, F. Driessens, and J. A. Planell, *J. Am. Ceram. Soc.*, 1999, **82**, 2808.
6. F. H. Lin, Ch. J. Liao, K. Sh. Chen, J. Sh. Sun, and Ch. P. Lin, *Biomaterials*, 2001, **22**, 2981.
7. L. Yubao, Zh. Xingdong, and K. De Groot, *Biomaterials*, 1997, **18**, 737.

Table 2. Results of the synthesis of hydroxyapatite from α -Ca₃(PO₄)₂ at 150–200 °C

Conditions		Products*		
<i>T</i> /°C	<i>t</i> /h	Phase composition	<i>L</i>	<i>d</i>
			μm	
150	2	α -Ca ₃ (PO ₄) ₂ + HAP	≤ 5	≤ 8
150	5	HAP		
175	2	α -Ca ₃ (PO ₄) ₂ + HAP**	≤ 8	≤ 1.5
175	5	HAP		
200	2	α -Ca ₃ (PO ₄) ₂ + HAP**	≤ 10	≤ 2.5
200	5	HAP**		

* Needles of length *L* and thickness *d*.

** The main phase of a mixture of the reaction products.

8. A. Bigi, E. Boanini, R. Botter, S. Panzaolta, and K. Rubini, *Biomaterials*, 2002, **23**, 1849.
9. K. S. TenHuisen and P. W. Brown, *Biomaterials*, 1998, **19**, 2209.
10. C. Durucan and P. W. Brown, *J. Mater. Sci.: Materials in Medicine*, 2000, **11**, 365.
11. C. Durucan and P. W. Brown, *J. Mater. Sci.*, 2002, **37**, 963.
12. S. Habelitz, L. Pascual, and A. Duran, *J. Mater. Sci.: Materials in Medicine*, 2002, **36**, 4131.
13. A. Nakahira and K. Sakamoto, *J. Am. Ceram. Soc.*, 1999, **82**, 2029.
14. K. Sakamoto, Sh. Yamaguchi, A. Nakahira, M. Kaneno, M. Okazaki, J. Ichihara, Y. Tsunawaki, and J. C. Elliott, *J. Mater. Sci.*, 2002, **37**, 1033.
15. A. Rodriguez and A. Lebugle, *Colloids Surfaces A: Physiochem. Eng. Aspects*, 1998, **45**, 191.
16. M. Tamai, T. Isshiki, K. Nishio, A. Nakahira, M. Nakamura, and H. Endoh, *J. Mater. Res.*, 2003, **18**, 2633.
17. K. S. TenHuisen and P. W. Brown, *J. Am. Ceram. Soc.*, 1999, **82**, 2813.
18. Yu. V. Kolen'ko, A. A. Burukhin, B. R. Churagulov, and N. N. Oleynikov, *Materials Letters*, 2003, **57**, 1124.
19. D. L. Parkhurst, D. C. Thorstenson, and L. N. Plummer, *PHREEQE — A Computer Program for Geochemical Calculations: U.S. Geological Survey Water-Resources Investigations Report*, 1980, 80–96, 195 p. (Revised and reprinted August, 1990.)
20. X. Yang and Zh. Wang, *J. Mater. Chem.*, 1998, **8**, 2233.
21. M. E. Brown, D. Dollimore, and A. K. Galwey, *Comprehensive Chemical Kinetics. Reactions in the Solid State*, Eds C. H. Bamford and C. F. H. Tipper, Elsevier Sci. Publ. Co., 1980, 22.
22. S. D. Langstaff, M. Sayer, T. J. N. Smith, S. M. Pugh, S. A. M. Hesp, and W. T. Thompson, *Biomaterials*, 1999, **20**, 1727.

*Received November 25, 2004;
in revised form December 24, 2004*